

Kinematics and Dynamics of a Three-Wheeled 2-DOF AGV

Subir Kumar Saha and Jorge Angeles

Department of Mechanical Engineering &
McGill Research Centre for Intelligent Machines, McGill University
817 Sherbrooke Street W., Montreal, Canada H3A 2K6

Abstract

In this paper a systematic method for the kinematic and dynamic modeling of a 2-dof Automatic Guided Vehicle (AGV) is presented. This type of methodology is useful to analyze, design, simulate and control any kind of rolling robots. The concept of *orthogonal complement* is used to develop the dynamical equations of motion. The vehicle is analyzed for simulation purposes. Simulation results are reported.

1. Introduction

The subject of this paper is the kinematics and dynamics of a 2-dof AGV for purposes of modeling, simulation and control. These are essential for the autonomous operation of AGVs. Current AGVs in industry follow predetermined paths, marked by reflective tape, paint or buried wire (Premi and Besant, 1983). The applications of AGVs without physical guidepaths, like dead reckoning, beacon systems, inertial navigation systems or computer vision systems (Boegli, 1985), can be extended to many other fields. These areas of application are space and undersea exploration (Tanaka, 1985), nuclear and explosive handling (Meieran and Gelhaus, 1986), security (Kajiwara et al., 1985), military (Lindauer and Hill, 1985), mobility for the disabled (Madarasz et al., 1986) and others (Moravec, 1983; Borenstein and Koren, 1985). Literature investigations reveal that, since the invention of automated guided vehicles, very limited attention has been paid to the development of methodologies for analyzing, designing, simulating and controlling mobile systems.

In contrast to robotic manipulators, which are holonomic systems, rolling robots are non-holonomic systems. The rolling constraints in the wheels make kinematic and dynamic analyses more complicated than those of holonomic systems. Recently, some work on kinematic modeling (Agulló et al., 1987; Muir and Neuman, 1987a & b) of AGVs has been reported. The application of those methods (Muir and Neuman, 1987a & b) to closed kinematic chains with conventional wheels increases the complexity in the modeling.

In this paper a simple method is introduced for kinematic modeling. Furthermore, the concept of *orthogonal*

complement (Angeles and Lee, 1988) of the matrix of non-holonomic constraints is used for the development of the dynamical equations of motion of the problem at hand.

2. Kinematic Analyses

It is assumed that the automated guided vehicle under study contains three wheels and a platform. Moreover, the platform is coupled by revolute pairs to the two rear wheels. Furthermore, only two rear wheels are driven or actuated by independent motors, and hence the vehicle has two degrees of freedom. Thus, the angular displacements of the actuated joints can be considered as the independent joint variables. For stability purposes, a caster wheel is attached at the front of the platform, as shown in Fig. 1, which is

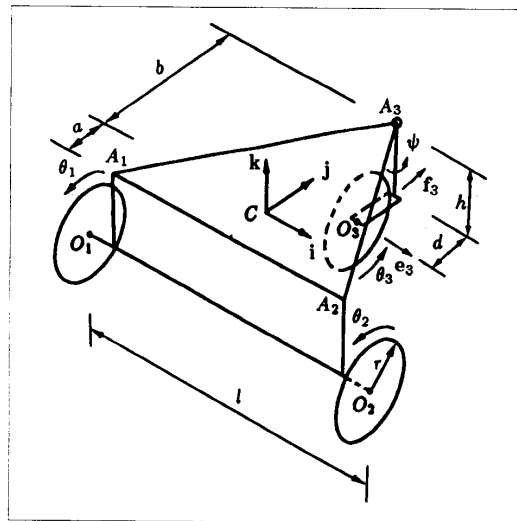


Figure 1 3D View of a 2-dof AGV.

free to attain any orientation according to the motion of the vehicle. For the kinematic analyses, a coordinate frame of unit vectors i, j, k is fixed at the centroid of the platform and e_i, f_i, g_i ($i = 1, 2, 3$) are attached to the centers of the wheels, numbered 1, 2 and 3. Here, according to the

definition of the architecture of the vehicle, axes e_i and f_i , for $i = 1, 2$, are parallel with i and j , respectively, and g_i coincides with k .

2.1 Velocity Analysis

According to Fig. 1, the velocity of point C can be written as:

$$\mathbf{v}_C = \dot{\mathbf{c}} = \mathbf{v}_{O_1} + \mathbf{v}_{C/O_1} \quad (1a)$$

where \mathbf{v}_{O_1} is velocity of point O_1 and \mathbf{v}_{C/O_1} is the relative velocity of C with respect to O_1 . \mathbf{v}_{O_1} can be written in terms of the radius, r , of the wheels and the spinning speed or actuated joint rate of the first wheel, $\dot{\theta}_1$, whose direction is positive in the counterclockwise direction about vector i , as:

$$\mathbf{v}_{O_1} = -\dot{\theta}_1 r \mathbf{j} \quad (1b)$$

and \mathbf{v}_{C/O_1} can be given as a cross product of the angular velocity, $\bar{\omega}$, of the vehicle with the vector, $\overline{O_1C}$, joining O_1 with C . This is as follows:

$$\mathbf{v}_{C/O_1} = \bar{\omega} \times \overline{O_1C} \quad (1c)$$

The angular velocity of the vehicle can be written from the joint rates of the driving wheels as:

$$\bar{\omega} = \frac{r}{l}(\dot{\theta}_1 - \dot{\theta}_2)\mathbf{k} \quad (2)$$

Now, using eqs.(1) and (2), an equation relating the velocity of the platform with the actuated joint rates is obtained as follows:

$$\mathbf{v}_C = \dot{\mathbf{c}} = -\frac{ar}{l}(\dot{\theta}_1 - \dot{\theta}_2)\mathbf{i} - \frac{r}{2}(\dot{\theta}_1 + \dot{\theta}_2)\mathbf{j} \quad (3)$$

where l and a , as shown in Fig. 1, are architecture dependent.

Combining eqs.(2) and (3), the *twist* \mathbf{t}_p of the platform, to be defined presently, is written as a linear transformation of the *actuated joint rate* vector, $\dot{\theta}_a$:

$$\mathbf{t}_p = \mathbf{T}_p \dot{\theta}_a \quad (4a)$$

where \mathbf{t}_p is a 6D vector of the angular velocity, $\bar{\omega}$, and the mass-center velocity, $\dot{\mathbf{c}}$, of the platform, $\dot{\theta}_a$ is a 2D vector and \mathbf{T}_p is 6×2 matrix. These are given as:

$$\mathbf{t}_p = [\bar{\omega}^T, \dot{\mathbf{c}}^T]^T, \quad \dot{\theta}_a = [\dot{\theta}_1, \dot{\theta}_2]^T \quad (4b)$$

$$\mathbf{T}_p = \frac{r}{l} \begin{bmatrix} \mathbf{k} & -\mathbf{k} \\ -a\mathbf{i} - \frac{l}{2}\mathbf{j} & a\mathbf{i} - \frac{l}{2}\mathbf{j} \end{bmatrix} \quad (4c)$$

2.2 Acceleration Analysis

To obtain the relation between the acceleration of the platform, or *twist rate*, and the actuated joint accelerations and rates, we differentiate the relation obtained in eq.(4a), with respect to time, which leads to

$$\dot{\mathbf{t}}_p = \mathbf{T}_p \ddot{\theta}_a + \dot{\mathbf{T}}_p \dot{\theta}_a \quad (5a)$$

where,

$$\dot{\mathbf{t}}_p = [\dot{\bar{\omega}}^T, \dot{\dot{\mathbf{c}}}]^T \quad \text{and} \quad \ddot{\theta}_a = [\ddot{\theta}_1, \ddot{\theta}_2]^T \quad (5b)$$

$\dot{\mathbf{T}}_p$, producing the centrifugal and Coriolis acceleration terms, is given as:

$$\dot{\mathbf{T}}_p = \frac{r^2}{l^2}(\dot{\theta}_1 - \dot{\theta}_2) \begin{bmatrix} \mathbf{0} & \mathbf{0} \\ \frac{l}{2}\mathbf{i} - a\mathbf{j} & \frac{l}{2}\mathbf{i} + a\mathbf{j} \end{bmatrix} \quad (5c)$$

2.3 Inverse Kinematics

Inverse kinematics is defined as: "given the cartesian positions and their derivatives, determine the joint histories".

Since the motion of the platform is planar, a 6D *twist* vector is unnecessary, for a 3D reduced *twist* will suffice. If vector \mathbf{t}_p is replaced by a 3D *twist* vector, \mathbf{t}_p' , defined in terms of the angular velocity component about \mathbf{k} , ω , the $\dot{\mathbf{c}}$ component along \mathbf{i} , \dot{x} , and the $\dot{\mathbf{c}}$ component along \mathbf{j} , \dot{y} , of the vehicle, then eq.(4a) can be rewritten as indicated below, provided that matrix \mathbf{T}_p is replaced by a corresponding 3×2 matrix \mathbf{T}_p' :

$$\mathbf{t}_p' = \mathbf{T}_p' \dot{\theta}_a \quad (6a)$$

where,

$$\mathbf{t}_p' = [\omega, \dot{x}, \dot{y}]^T \quad \text{and} \quad \mathbf{T}_p' = \frac{r}{l} \begin{bmatrix} 1 & -1 \\ -a & a \\ -\frac{l}{2} & -\frac{l}{2} \end{bmatrix} \quad (6b)$$

The joint rates can be obtained by regarding eq.(6a) as an overdetermined system of three equations in two unknowns. The least-square approximation of this system is given as:

$$\dot{\theta}_a = \mathbf{T}_p'^I \mathbf{t}_p' \quad (6c)$$

where, $\mathbf{T}_p'^I = (\mathbf{T}_p'^T \mathbf{T}_p')^{-1} \mathbf{T}_p'^T$ is the Moore-Penrose generalized inverse of \mathbf{T}_p' .

Similarly, for acceleration inversion, if the 6D *twist rate* vector, $\dot{\mathbf{t}}_p$ is replaced by a 3D vector, $\dot{\mathbf{t}}_p'$, and the 6×2 matrix, \mathbf{T}_p is replaced by the 3×2 matrix, \mathbf{T}_p' , then eq.(5a) is rewritten as:

$$\dot{\mathbf{t}}_p' = \mathbf{T}_p' \ddot{\theta}_a + \dot{\mathbf{T}}_p' \dot{\theta}_a \quad (7a)$$

where,

$$\dot{\mathbf{t}}_p' = [\dot{\omega}, \dot{\dot{x}}, \dot{\dot{y}}]^T \quad \text{and} \quad \dot{\mathbf{T}}_p' = \frac{r^2}{l^2}(\dot{\theta}_1 - \dot{\theta}_2) \begin{bmatrix} \mathbf{0} & \mathbf{0} \\ \frac{l}{2} & \frac{l}{2} \\ -a & a \end{bmatrix} \quad (7b)$$

It is to be noted that eq.(7a) can also be obtained by differentiating eq.(6a) as:

$$\dot{\mathbf{t}}'_p = \mathbf{T}_p \ddot{\theta}_a + \mathbf{W}_p \mathbf{T}_p \dot{\theta}_a \quad \text{where } \mathbf{W}_p = \begin{bmatrix} 0 & 0 & 0 \\ 0 & 0 & -\omega \\ 0 & \omega & 0 \end{bmatrix} \quad (7c)$$

\mathbf{W}_p is a 3×3 transformation matrix which takes into account the motion of the coordinate frame $\mathbf{i}, \mathbf{j}, \mathbf{k}$.

Now, actuated joint accelerations are computed from eq.(7a) as:

$$\ddot{\theta}_a = \mathbf{T}_p^{-1} [\dot{\mathbf{t}}'_p - \mathbf{T}_p \dot{\theta}_a] \quad (7d)$$

To obtain the actuated joint angles, $\bar{\theta}_a = [\theta_1, \theta_2]^T$, eqs.(6c), which relate the Cartesian velocities with joint rates, are integrated, with known initial conditions, by any standard integration scheme.

2.4 Direct Kinematics

As opposed to inverse kinematics, direct kinematics is defined as: "given the joint variables and their derivatives, determine the position, velocity and acceleration of each body of the system".

Velocities and accelerations can be easily computed from eqs.(6) and (7). But to obtain the positions, which is essential to control the location of the vehicle, the twist relation in (6a) is written in the fixed coordinate frame in component form as:

$$\omega = \frac{r}{l} (\dot{\theta}_1 - \dot{\theta}_2) \quad (8a)$$

$$\dot{X} = \dot{x} \cos \beta - \dot{y} \sin \beta \quad (8b)$$

$$\dot{Y} = \dot{x} \sin \beta + \dot{y} \cos \beta \quad (8c)$$

where β is the angle between the moving frame of unit vectors $\mathbf{i}, \mathbf{j}, \mathbf{k}$ (Fig. 1) and the fixed frame, as shown in Fig. 3a. Moreover, \dot{X} and \dot{Y} are the \dot{c} components along the X and Y directions of the fixed coordinate frame, respectively. Clearly, eqs.(8b & c) are the nonholonomic constraints of the system.

With the known initial positions and input $\ddot{\theta}_a$, positions of the vehicle at any time can be obtained by integrating eqs.(8).

3. Dynamic Analyses

3.1 Computation of the Natural Orthogonal Complement and Derivation of Equations of Motion

As pertaining to mechanical systems composed of constrained rigid bodies, the natural orthogonal complement of the matrix of velocity constraints can be computed as follows:

Step 1: The *twist* of a rigid body undergoing an arbitrary motion in the 3D space, \mathbf{t} , is defined as indicated in

eq.(4b) for the platform. Moreover, if \mathbf{I} denotes the *inertia tensor* of a rigid body about its mass center, and this, as well as all vector quantities involved, are referred to a coordinate system fixed to the body, then, the Newton-Euler equations governing the motion of the body are written as follows:

$$\mathbf{M} \dot{\mathbf{t}} = -\mathbf{W} \mathbf{M} \mathbf{t} + \mathbf{w} \quad (10)$$

where the *wrench* \mathbf{w} acting on the body is defined, in accordance with the definition of \mathbf{t} , as:

$$\mathbf{w} \equiv [\mathbf{n}^T, \mathbf{f}^T]^T \quad (11)$$

\mathbf{n} and \mathbf{f} denoting the resultant torque and the resultant force acting at the mass center of the body. Now, tensor $\mathbf{\Omega}$ is defined as:

$$\mathbf{\Omega} \equiv \frac{\partial(\bar{\omega} \times \mathbf{x})}{\partial \mathbf{x}} \equiv \bar{\omega} \times \mathbf{1} \quad (12a)$$

for an arbitrary 3D vector \mathbf{x} , whereas the 6×6 matrices of *extended angular velocity*, \mathbf{W} , and of *extended mass*, \mathbf{M} , are defined in turn as:

$$\mathbf{W} \equiv \begin{bmatrix} \mathbf{\Omega} & \mathbf{0} \\ \mathbf{0} & \mathbf{0} \end{bmatrix}, \quad \mathbf{M} \equiv \begin{bmatrix} \mathbf{I} & \mathbf{0} \\ \mathbf{0} & m \mathbf{1} \end{bmatrix} \quad (12b)$$

where m , $\mathbf{0}$ and $\mathbf{1}$ denote the mass of the rigid body, the zero and the identity tensors, respectively.

Step 2: It is assumed that the mechanical system under motion is composed of p rigid bodies. Now, the Newton-Euler equations for the i th body can be written as:

$$\mathbf{M}_i \dot{\mathbf{t}}_i = -\mathbf{W}_i \mathbf{M}_i \mathbf{t}_i + \mathbf{w}_i^E + \mathbf{w}_i^C, \quad i = 1, \dots, p \quad (13)$$

where \mathbf{w}_i^E and \mathbf{w}_i^C are external and the nonworking constraint wrenches acting on the same body, respectively. Next, the $6p \times 6p$ matrices of *generalized mass*, \mathbf{M} , and of *generalized angular velocity*, \mathbf{W} , as well as the $6p$ -dimensional vectors of *generalized twist*, \mathbf{t} , of *generalized external wrench*, \mathbf{w}^E , and *generalized, nonworking constraint wrench*, \mathbf{w}^C , are defined as:

$$\mathbf{M} \equiv \text{diag}[\mathbf{M}_1, \mathbf{M}_2, \dots, \mathbf{M}_p] \quad (14a)$$

$$\mathbf{W} \equiv \text{diag}[\mathbf{W}_1, \mathbf{W}_2, \dots, \mathbf{W}_p] \quad (14b)$$

$$\mathbf{t} \equiv \begin{bmatrix} \mathbf{t}_1 \\ \mathbf{t}_2 \\ \vdots \\ \mathbf{t}_p \end{bmatrix}, \quad \mathbf{w}^E \equiv \begin{bmatrix} \mathbf{w}_1^E \\ \mathbf{w}_2^E \\ \vdots \\ \mathbf{w}_p^E \end{bmatrix}, \quad \mathbf{w}^C \equiv \begin{bmatrix} \mathbf{w}_1^C \\ \mathbf{w}_2^C \\ \vdots \\ \mathbf{w}_p^C \end{bmatrix} \quad (14c)$$

Hence, the p dynamical equations (13) can now be expressed in compact form as follows:

$$\mathbf{M} \dot{\mathbf{t}} = -\mathbf{W} \mathbf{M} \mathbf{t} + \mathbf{w}^E + \mathbf{w}^C \quad (15)$$

which is an equation formally identical to eq.(10), and constitutes a set of $6p$ *unconstrained* dynamical equations.

Step 3: The kinematic constraints produced by nonholonomic couplings are derived in differential form. Within the methodology adopted here, a nonholonomic constraint

has three scalar equations, as opposed to a holonomic constraint, which gives rise to six scalar equations. Moreover, the said constraints can be represented as a system of linear homogeneous equations on the twists. This is equivalent to the following linear system on the vector of *generalized twist*:

$$\mathbf{A}\mathbf{t} = \mathbf{0} \quad (16)$$

Here, \mathbf{A} is a $(6\gamma+3\nu) \times 6p$ matrix, γ and ν being the number of *independent* holonomic and nonholonomic constraints, respectively.

Under the assumption that the degree of freedom of the system is n , a n -dimensional vector $\dot{\theta}_a$ of *independent or actuated generalized speeds* is defined. Then, the vector of *generalized twist* can be represented as the following linear transformation of $\dot{\theta}_a$:

$$\mathbf{t} = \mathbf{T}\dot{\theta}_a \quad (17)$$

where \mathbf{T} is a $6p \times n$ matrix. Upon substitution of \mathbf{t} , as given by eq.(17), into eq.(16), the following is readily derived:

$$\mathbf{A}\mathbf{T} = \mathbf{0} \quad (18)$$

which shows that \mathbf{T} is an *orthogonal complement* of \mathbf{A} .

Step 4: Because of the definitions of \mathbf{A} and the vector of nonworking constraint wrench, the latter turns out to lie in the range of the transpose of \mathbf{A} and hence, the said wrench lies in the nullspace of the transpose of \mathbf{T} . Therefore, upon multiplication of both sides of the $6p$ -dimensional Newton–Euler uncoupled equations of the system, eq.(15), by the transpose of \mathbf{T} , the vector of nonworking constraint wrench is eliminated from the said equation, which leads to:

$$\mathbf{T}^T \mathbf{M}\dot{\mathbf{t}} = -\mathbf{T}^T \mathbf{W}\mathbf{M}\mathbf{t} + \mathbf{T}^T \mathbf{w}^E \quad (19)$$

Now, both sides of eq.(17) are differentiated with respect to time, which yields

$$\dot{\mathbf{t}} = \mathbf{T}\ddot{\theta}_a + \dot{\mathbf{T}}\dot{\theta}_a \quad (20)$$

Furthermore, \mathbf{w}^E is decomposed as follows:

$$\mathbf{w}^E = \mathbf{w}^J + \mathbf{w}^G + \mathbf{w}^D \quad (21)$$

where \mathbf{w}^J , \mathbf{w}^G and \mathbf{w}^D represent generalized wrenches due to torques and forces applied at the joints, due to gravity, and due to dissipative torques and forces, respectively.

Upon substitution of eqs.(20) and (21) into eq.(19), the following system of n independent constrained dynamical equations is derived:

$$\mathbf{T}^T \mathbf{M}\mathbf{T}\ddot{\theta}_a = -\mathbf{T}^T (\mathbf{M}\dot{\mathbf{T}} + \mathbf{W}\mathbf{M}\mathbf{T})\dot{\theta}_a + \mathbf{T}^T (\mathbf{w}^J + \mathbf{w}^G + \mathbf{w}^D)$$

or,

$$\mathbf{I}(\ddot{\theta})\dot{\theta}_a = \mathbf{C}(\ddot{\theta}, \dot{\theta}_a)\dot{\theta}_a + \bar{\tau} + \bar{\gamma} + \bar{\delta} \quad (22)$$

where $\ddot{\theta}$ is a vector consisting of independent or actuated and dependent or unactuated coordinates; $\mathbf{I} \equiv \mathbf{T}^T \mathbf{M}\mathbf{T} \equiv$

$n \times n$ matrix of generalized inertia; $\mathbf{C} \equiv -\mathbf{T}^T (\mathbf{M}\dot{\mathbf{T}} + \mathbf{W}\mathbf{M}\mathbf{T}) \equiv n \times n$ matrix of convective inertia terms; $\bar{\tau} \equiv \mathbf{T}^T \mathbf{w}^J \equiv n$ -dimensional vector of generalized driving force; $\bar{\gamma} \equiv \mathbf{T}^T \mathbf{w}^G \equiv n$ -dimensional vector of generalized force due to gravity and $\bar{\delta} \equiv \mathbf{T}^T \mathbf{w}^D \equiv n$ -dimensional vector of generalized dissipative force.

From the foregoing, then, it becomes apparent that eqs.(22) represent the system's Euler–Lagrange dynamical equations, which appear, moreover, free of constraint forces.

3.2 Inverse dynamics

It is assumed that the system at hand consists of five rigid bodies. The bodies are numbered 1 to 5 as shown in Fig. 2.

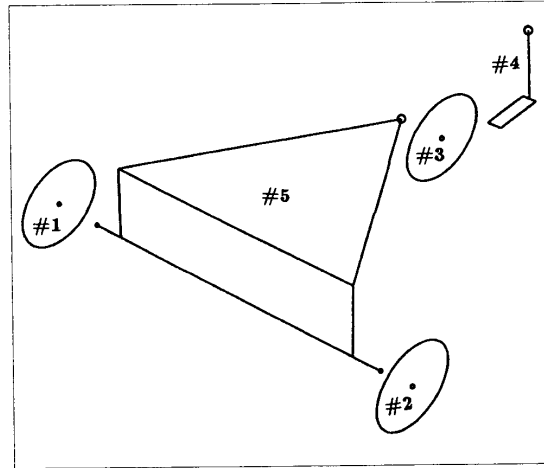


Figure 2 Disassembled Vehicle.

With the actuated joint-angle and joint-rate vectors, other two vectors, the unactuated joint-angle and joint-rate vectors are defined as:

$$\bar{\theta}_u = [\theta_3, \psi]^T \quad \text{and} \quad \dot{\bar{\theta}}_u = [\dot{\theta}_3, \dot{\psi}]^T \quad (23)$$

where θ_3 , ψ and $\dot{\theta}_3$, $\dot{\psi}$ are joint angles and rates of the third-wheel rolling and yaw, respectively. Next, the *twist* of each individual body is written as a linear transformation of all joint rates, i.e.,

$$\mathbf{t} = \mathbf{T}_a \dot{\bar{\theta}}_a + \mathbf{T}_u \dot{\bar{\theta}}_u \quad (24a)$$

Here \mathbf{t} is a 30D vector, defined as:

$$\mathbf{t} = [\mathbf{t}_1^T, \dots, \mathbf{t}_5^T]^T \quad (24b)$$

\mathbf{T}_a and \mathbf{T}_u being 30×2 matrices associated with actuated and unactuated joint rates, respectively.

Since there are only two independent joint rates, we need a relation between unactuated joint rates and actuated joint rates. This can be obtained by writing the velocity of point O_3 from the velocity of point O_1 as:

$$\mathbf{v}_{O_3} = \mathbf{v}_{O_1} + \omega \mathbf{k} \times \overline{O_1 A_3} + (\omega + \dot{\psi}) \mathbf{k} \times \overline{A_3 O_3} \quad (25a)$$

where \mathbf{v}_{O_3} is velocity of the point O_3 , $\overline{O_1 A_3}$ and $\overline{A_3 O_3}$ are vectors from O_1 to A_3 and A_3 to O_3 , respectively. After simplification, eq.(25a) leads to

$$\mathbf{J}_a \dot{\theta}_a + \mathbf{J}_u \dot{\theta}_u = 0 \quad (25b)$$

where \mathbf{J}_a and \mathbf{J}_u are 2×2 matrices. A similar relation is also obtained if we write the velocity of O_3 from the velocity of O_2 . From eq.(25b) the unactuated joint rates are obtained as:

$$\dot{\theta}_u = -\mathbf{J}_u^{-1} \mathbf{J}_a \dot{\theta}_a \quad (26)$$

which are always possible to calculate, for \mathbf{J}_u never becomes singular. In fact, it turns out that $\det(\mathbf{J}_u) = -rd$.

Now, the generalized twist, \mathbf{t} , can be written in terms of the independent generalized joint rates, $\dot{\theta}_a$, as:

$$\mathbf{t} = \mathbf{T} \dot{\theta}_a \quad \text{where} \quad \mathbf{T} = \mathbf{T}_a - \mathbf{T}_u \mathbf{J}_u^{-1} \mathbf{J}_a \quad (27)$$

Moreover, the generalized twist rate is:

$$\dot{\mathbf{t}} = \mathbf{T} \ddot{\theta}_a + \dot{\mathbf{T}} \dot{\theta}_a \quad (28a)$$

where

$$\dot{\mathbf{T}} = \dot{\mathbf{T}}_a - \dot{\mathbf{T}}_u \mathbf{J}_u^{-1} \mathbf{J}_a + \mathbf{T}_u \mathbf{J}_u^{-1} \dot{\mathbf{J}}_u \mathbf{J}_u^{-1} \mathbf{J}_a - \mathbf{T}_u \mathbf{J}_u^{-1} \dot{\mathbf{J}}_a \quad (28b)$$

Using equations (27) and (28), eq.(22) can be written as:

$$\mathbf{I}(\ddot{\theta}) \ddot{\theta}_a = \mathbf{C}(\ddot{\theta}, \dot{\theta}_a) \dot{\theta}_a + \bar{\tau} + \bar{\delta} \quad (29)$$

where $\ddot{\theta} = [\ddot{\theta}_a^T, \ddot{\theta}_u^T]^T$, \mathbf{I} and \mathbf{C} being 2×2 matrices, $\bar{\tau}$ and $\bar{\delta}$ are 2D vectors.

For inverse dynamics, eq.(29) is used to compute the required actuator-torques.

3.3 Direct dynamics

Direct dynamics involves the integration of the equations of motion, eq.(29). Any standard routine can be used to do this. For the problem discussed here the DVERK subroutine of IMSL, which solves first-order differential equations by the Runge-Kutta 5th/6th order method, is used.

Equation (29) is written in first-order form as follows:

$$\dot{\mathbf{q}} = \mathbf{P} \mathbf{q} + \mathbf{Q} \mathbf{u} \quad (30)$$

where

$$\mathbf{q} = [\theta_1, \theta_2, \dot{\theta}_1, \dot{\theta}_2]^T \quad \text{and} \quad \mathbf{u} = \tau = [\tau_1, \tau_2]^T$$

Moreover, \mathbf{P} and \mathbf{Q} are the following 4×4 and 4×2 matrices

$$\mathbf{P} = \begin{bmatrix} \mathbf{0}_{2 \times 2} & \mathbf{1}_{2 \times 2} \\ \mathbf{0}_{2 \times 2} & \mathbf{I}^{-1} \mathbf{C} \end{bmatrix} \quad \mathbf{Q} = \begin{bmatrix} \mathbf{0}_{2 \times 2} \\ \mathbf{I}^{-1} \end{bmatrix}$$

4. Numerical Example

For numerical purposes, the geometrical parameters of the vehicle are considered as:

$$l = .4\text{m}, r = .05\text{m}, a = .1010\text{m}, \\ b = .2020\text{m}, d = .025\text{m} \text{ and } h = .1\text{m}.$$

The inertial parameters are considered as:

Mass of each wheel = 2kg.

Inertia tensor for each wheel.

$$\mathbf{I}_i = \text{diag} [.0025, .00125, .00125] \text{kgm}^2 \quad \text{for } i = 1, 2, 3$$

Mass of the platform = 20kg.

Inertia tensor of the platform.

$$\mathbf{I}_5 = \text{diag} [0.7083, 0.7083, 0.4083] \text{kgm}^2$$

Compared to the mass of the wheels and the platform, the mass of the link connected with the front wheel (fourth body) is considered negligible.

The vehicle is programmed to traverse a circular path of radius R , as shown in Fig. 3(a), in 60s. The sweep angle β is assumed to be a fifth-order polynomial function of time verifying zero velocity and acceleration conditions at start and end points. This is given as:

$$\beta(t) = a_0 + a_1 t + \dots + a_5 t^5$$

with the following numerical values:

$$a_0 = 0.0, a_1 = 0.0, a_2 = 0.0, a_3 = \frac{20\pi}{60^3}$$

$$a_4 = -\frac{30\pi}{60^4} \text{ and } a_5 = \frac{12\pi}{60^5}$$

where a_i is measured in units of rad/s^i , for $i=0,1,\dots,5$. The variation of β with time is shown in Fig. 3(b).

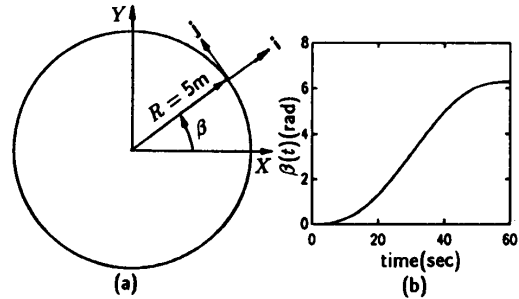


Figure 3 (a) Trajectory. (b) Variation of β with time.

The results obtained from inverse kinematics and dynamics are shown in Figs. 4. The simulation errors for joint variables are shown in Fig. 5.

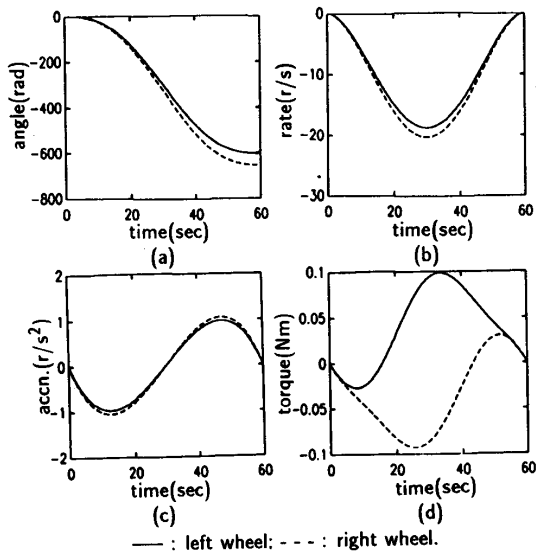


Figure 4 Required Joint (a) Angles, (b) Rates, (c) Accelerations and (d) Torques.

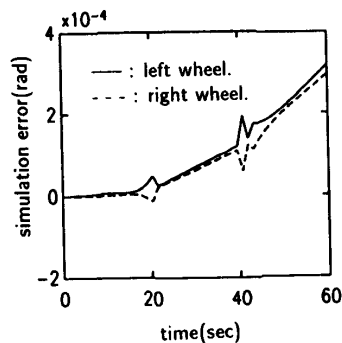


Figure 5 Simulation Errors in Joint Angles.

5. Conclusions

We have shown that, using the natural orthogonal complement of the matrix of velocity constraint equations, it is possible to derive systematically the Euler-Lagrange equations of motion of nonholonomic robotic mechanical systems. Moreover, the introduction of the said orthogonal complement leads naturally to an efficient computational algorithm. The integration errors found in the numerical example are due only to truncation errors in the integration routine. In fact, we tried tighter tolerances, from 10^{-1} to 10^{-5} , and the error did not decrease substantially. Nevertheless, for practical purposes, the errors produced by the integration routines are quite acceptable.

6. Acknowledgements

The research work reported here was possible under NSERC Grant No. A4532 and FCAR(Fonds pour la formation de chercheurs et l'aide à la recherche, Québec) Grant No. 88A525A. The scholarship granted to Subir Kumar Saha by the Government of India is highly acknowledged.

7. References

- Agulló, J., Cardona, S., and Vivancos, J., 1987, "Kinematic of vehicles with directional sliding wheels", *Mech. and Mach. Th.*, Vol. 22, No. 4, pp. 295-301.
- Angeles, J., and Lee, S., 1988, "The formulation of dynamical equations of holonomic mechanical systems using a natural orthogonal complement", *Trans. of the ASME, J. of Appl. Mech.*, Vol. 55, March, pp. 243-244.
- Boegli, P., 1985, "A comparative evaluation of AGV navigation techniques", *Proc. of the 3rd Int. Conf. on AGVS*, Stockholm, Sweden, Oct. 15-17, pp. 169-180.
- Borenstein, J., and Koren, Y., 1985, "A mobile platform for nursing robots", *IEEE Trans. on Ind. Electronics*, Vol. 32, No. 2, May, pp. 158-165.
- Kajiwara, T., Yamaguchi, J., Kanayama, Y., Yuta, S., Iijima, J., Imasato, K., and Uehara, T., 1985, "Development of a mobile robot for security guard", *Proc. of the 15th Int. Symp. on Ind. Robots*, Tokyo, Japan, Sept. 11-13, Vol. 1, pp. 271-278.
- Lindauer, B., and Hill, J.D., 1985, "Military robotics: an overview", *Robotics Age*, Nov., pp. 16-21.
- Madarasz, R.L., Heiny, L.C., Cromp, R.F., and Mazur, N.M., 1986, "The design of an autonomous vehicle for the disabled", *IEEE J. of R & A*, Vol. RA-2, No. 3, Sept., pp. 117-126.
- Meieran, H.B., and Gelhaus, F.E., 1986, "Mobile robots designed for hazardous environments", *Robotics Eng.*, March, pp. 10-16.
- Moravec, H.P., 1983, "The Stanford cart and the CMU rover", *Proc. of the IEEE*, Vol. 71, No. 7, pp. 872-884.
- Muir, P.F., and Neuman, C.P., 1987a, "Kinematic modeling for feedback control of an omnidirectional wheeled mobile robot", *Proc. of the IEEE Conf. on R & A*, Raleigh, North Carolina, March 31-April 3, pp. 1772-1778.
- Muir, P.F., and Neuman, C.P., 1987b, "Kinematic modeling of wheeled mobile robots", *J. of Robotic Systems*, Vol. 4, No. 2, pp. 281-340.
- Premi, S.K., and Besant, C.B., 1983, "A review of various vehicle guidance techniques that can be used by mobile robots or AGVS", *Proc. of the 2nd Int. Conf. on AGVS*, Stuttgart, W. Germany, June 7-9, pp. 195-209.
- Tanaka, N., 1985, "The concept of the advanced robot for support of offshore oil exploration", *Proc. of the Int. Conf. on Adv. Robotics*, Tokyo, Japan, Sept. 9-10, pp. 507-511.